Fabrication and Characterisation of a Microfluidic Device for Bead-array Analysis by the LIBWE Method

Thomas Gumpenberger, Tadatake Sato, Aiko Narazaki, Yoshizo Kawaguchi, Ryozo Kurosaki and Hiroyuki Niino

Photonic Research Institute, National Institute of Advanced Industrial Science and Technology (AIST), AIST Tsukuba Central 5, 1-1-1 Higashi, Tsukuba, Ibaraki 305 8565, Japan
E-mail: sato-tadatake@aist.go.jp

We have developed a novel design for a microfluidic device incorporating a two-dimensional microbead array by using silica glass plates structured by the laser-micromachining method, **L**aser-**I**nduced **B**ackside **W**et **E**tching (LIBWE). Surface functionalized borosilicate glass and polymer microbeads 10 μm in diameter, which act as detectors, were fixed in etched microstructures and sealed with a polydimethylsiloxane plate to form a microfluidic system. The beads are regularly arranged in a two-dimensional manner without being in contact with any other. Analytes are supplied as a solution flowing in microchannels. The pressure-driven flow in the microchannels was investigated. The successful capture of fluorescein isothiocyanate by amino groups as well as that of biotin by avidin on the beads' surface was confirmed by fluorescence microscopy.

DOI: 10.2961/jlmn.2006.03.0010
Keywords: Laser-micromachining, LIBWE, microfluidic system, bioarray analysis, microbead

1. Introduction

Devices incorporating microchannels and other microfluidic structures have recently attracted increased interest. Potential applications range from micro-reactors, including portable fuel cells [1-4], to various kinds of analytical systems [5-7]. Micro total analysis systems (μTAS), also called “lab on a chip”, are widely studied for use in the separation, detection, and analysis of various chemical reagents [8]. These systems can offer potential advantages relative to conventional macroscopic instrumentation such as (i) reduced sample and reagent consumption, (ii) shorter analysis time, and (iii) higher sensitivity.

Surface-modified microbeads have been used occasionally in such microfluidic devices because it is easy to introduce several capturing functions to the device [9-10]. In these systems, biological probe molecules are immobilized on the surface of the beads, which range from several hundred nanometers to some tens of micrometers, to capture target molecules in a sample solution. The increased surface area induced by using microbeads can increase the sensitivity of the system. Such surface-modified microbeads can be used in bio-array analyses. Bio-arrays have been studied for the analysis of samples for a wide range of components in parallel with high throughput. In particular, DNA microarrays prepared on glass plates by spotting or photolithographic methods have already been used commercially [11-12]. However, serious challenges still remain, such as cost-effective production of the device and a reduction in the reaction time.

Bead-based systems have been developed as a technique to meet the first challenge because they can be mass-produced by conventional synthetic procedures. Several analysis techniques utilizing microbeads have been developed: (1) The combination of color-coded microbeads and a flow cytometer [13-14]; (2) the massive parallel signature sequence, which uses microbeads for cDNA cloning and parallel sequencing reaction [15-16]; and (3) fixed microbeads loaded into a microwell-array fabricated at the terminal end of a fiberoptic bundle [17-19]. Walt and co-workers have developed a system called a random array, where randomly arranged microbeads are addressed by fluorescent signals encoded to each microbead.

The other remaining challenge in bio-array analysis is the reduction of analysis time. As described previously, a microfluidic system can address this. There are several devices utilizing bead arrays under microfluidic conditions. Kohara et al. used a capillary to fix microbeads, thus forming a one-dimensional array [20-21]. Meanwhile, McDevitt and co-workers arranged microbeads into a microwell array fabricated by anisotropical etching of a silicon wafer. An optical tweezer was used to arrange the beads in an addressable fashion [22-23]. These devices proved that DNA hybridization can be achieved in a shorter reaction time and that a quite small amount of sample can be detected.

In these systems, a mechanism to fix the beads is indispensable because one needs to facilitate the readout of the (fluorescent) signals. For the fixing mechanism, Kohara and coworkers used a glass capillary, whereas McDevitt and coworkers used a microwell array prepared by anisotropical etching of a silicon wafer. These sample holders limit the size of the beads. Beads with diameters larger than 100 μm were used in these devices. Therefore, a key technology for the fabrication of novel bead-array

devices is a technique for micromachining. We have recently developed a laser micromachining technique for transparent materials, named Laser-Induced Backside Wet Etching (LIBWE) [24-25]. This technique uses the laser ablation of an organic solution that is in contact with the rear surface of a transparent sample material. This technique is based on mask projection but does not utilize resists and can be used under atmospheric conditions. Microstructures on transparent materials facilitate observation of inside phenomena by microscopes. By using silica glass, optical functions using ultraviolet (UV) light can be integrated onto the same device. Additionally, based on the robustness and chemical inertness of silica glass, sterilization and cleaning by using autoclaves and/or UV light becomes possible. This would enhance the reusability of fabricated devices.

We have developed a novel microfluidic device combining a bead array with microchannels and reported briefly [26]. The microstructure, which can be used as microchannels for sample transport as well as for fixing the microbeads, was fabricated by LIBWE. In this article, the preparation and operation of the device are reported in detail.

2. Experimental

2.1 Surface chemistry of the microbeads

Microbeads with a surface amino group were prepared from borosilicate glass beads (10 μm diameter, Duke Scientific Corporation) by a procedure similar to one reported earlier [27]. Before silanization, the beads were cleaned using NaOH, HCl/MeOH (1:1), and concentrated H_2SO_4. After each washing process, the washing medium was removed by centrifugation, and the beads were rinsed with distilled water. After the final washing, cleaned beads were dried under vacuum. Cleaned beads were silanized under a nitrogen atmosphere with an anhydrous toluene solution (approx. 2 mM) of *N*-(2-aminoethyl)-3-amino-propyltrimethoxysilane (AEAPS) for 3 h. After the reaction, beads were collected by filtration using membrane filters (Millipore Type JA 1.0 μm), and were then stored in deionized water containing about 0.1% Tween20 to prevent coalescing. Prepared beads were used within 2 weeks.

Microbeads with surface-immobilized avidin were prepared from polystyrene (PS) microbeads with surface carboxyl groups (10 μm diameter, 2.68% solid, Polyscience). A stock suspension of the beads (150 μL) was washed with distilled water and 0.1M NaH_2PO_4 (pH 6.2 ± 0.2). To the beads suspended in 0.1M NaH_2PO_4, 10 μL of *N*-hydroxysulfosuccinimide sodium salt (Sulfo-NHS) aqueous solution (50 mg in 1 mL) and 10 μL of 1-ethyl-3-(3-dimethylaminopropyl)carbodiimide hydrochloride (EDC-HCl) aqueous solution (100 mg in 1 mL) were added stepwise. Then the suspension was incubated for 20 min at room temperature (RT) with rotation (60 rpm). After incubation, the beads were collected by centrifugation and resuspended in a PBS buffer (pH 7.4). Avidin dissolved in PBS (0.51 mg in 500 μL) was added, and the solution rotated for 2 h. Then the suspension was treated with 1-aminoethanol solution for 30 min to terminate unreacted carboxyl groups. The obtained beads were stored in a PBS-TBN buffer (PBS containing 0.02% Tween20, 0.1% BSA, and 0.05% sodium azide). Before an experiment, the suspension was refrigerated at 4°C for up to 2 weeks.

2.2 Micromachining of the silica glass plate

Microstructures for fixing microbeads were fabricated on synthetic silica glass plates (2 cm square and 2 mm thickness) by the LIBWE method [24-25, 27] The 1 × 1 mm² microstructure areas were etched in a single step by mask projection. In the LIBWE method, the etch depth is controlled by the number of laser pulses. We obtained microstructures with depths of approximately 13 μm by irradiation with approximately 3000 pulses. Additional channels and holes used for liquid transfer were fabricated by the LIBWE method and an ultrasonic drill (Ultrasonic Engineering Co., USM-150N25S).

2.3 Device setup and capturing reaction

To form channels, a polydimethylsiloxane (PDMS) plate of 2 mm thickness was placed on top of the surface-micromachined silica glass plate. The PDMS plates were prepared by mixing PDMS prepolymer and a curing agent (Sylgard184, Dow Corning) in a 10:1 ratio (v/v), which were cured in a gap structure prepared by acrylic plates overnight at RT. On the holes at the surface of a silica glass plate (the reverse side of the PDMS plate), polyetheretherketone (PEEK) tubing with a 500 μm inner diameter was connected by a commercially available lock and screw system (Nanoport, Upcharch Scientific). These ports were glued on the surface of the silica glass. To supply reagents to the device, we employed a syringe pump system (KD Scientific Inc, Model 210). A pressure gauge (Keyence AP13S) was placed halfway between the pump and the chip-inlet to monitor the liquid pressure. Fluorescent images were recorded by using an inverted fluorescence microscope (Nikon TE-2000) equipped with a high-pressure mercury lamp (Nikon, Model C-SHG1), a filter wheel system (ProScan, Prior Scientific), and a CCD camera (Hamamatsu, ORCA-AG). Wavelength regions for excitation and emission were selected by band-pass filters mounted on the filter-wheel system: we used two filters, one for excitation (centre 490 nm/FWHM 20 nm) and one for emission (528 nm/38 nm) suitable for the detection of fluorescence signals from fluorescein derivatives. Beads were counted, and their fluorescence intensity values were evaluated by means of image analysis software (ImageProPlus 5.0). Normally, the total exposure time for the whole experimental processes was less than 2 min. It was confirmed that fluorescence intensities of fluorescein derivatives stayed above 90% of the original value under such exposure conditions.

3. Results and Discussion

3.1 Micromachining of silica glass

The pattern of the microstructure for fixing microbeads (Fig. 1) consisted of 32 parallel lines (1 mm length) with 50

cavities. From an SEM micrograph of the cross-section of a microstructure (Fig. 2), the depth of the channels was estimated to be 13 μm. The size of the structure is shown in Figure 1(b). The volume of each cavity is 2.7 pL. Inside a cavity, a bead with a diameter of 10 μm (V = 0.52 pL) occupies 19.4% of the volume. The remaining 2.2 pL is space for the sample solution. Microstructures with an area of 1 × 1 mm^2 could be prepared one at a time by LIBWE. The procedure was repeated four times to fabricate a 2 × 2 mm^2 arrangement (Fig. 3).

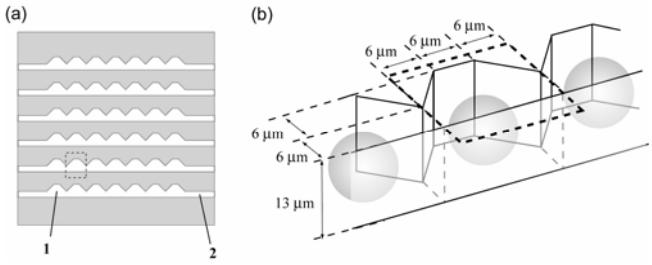

Fig. 1 Schematic drawing of the microstructure fabricated by LIBWE. (a) Overall pattern in a 1 × 1 mm^2 area, **1**: cavity for fixing a microbead, **2**: microchannels for connection. (b) Size of the etched cavity (area shown as a square with broken lines in (a)).

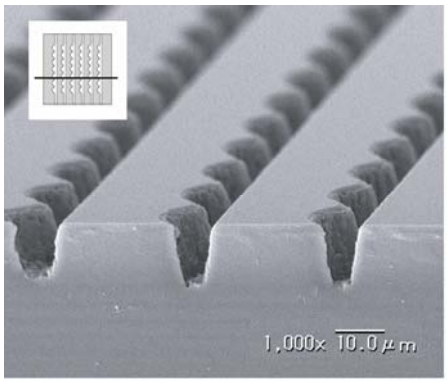

Fig. 2 An SEM image of the cross-section of an etched microstructure. A silica glass plate with microstructures was cut as indicated in the inset.

In addition, channels connecting the microstructures with inlet and outlet holes were fabricated on the same plate (Fig. 3). Using these channels, chemical reagents are supplied to and removed from the microstructure containing the microbeads. Shallow channels with 1 mm width and 40 μm depth, which were directly connected to the microstructures, were prepared by the LIBWE method in the same batch for preparing the microstructures. We hereafter call these "LIBWE channels." The LIBWE channels were prepared by scanning the etched area (1 × 1 mm^2) with pulsed laser irradiation. The depth of the LIBWE channels was controlled by varying the scanning rate at a fixed pulse repetition rate. Moreover, deep channels with 0.5 mm width and 600 μm depth, which were fabricated with an ultrasonic drill, connected the LIBWE channels and through-holes of 1 mm diameter, which were also fabricated with an ultrasonic drill. A micrograph of the microstructures on the silica glass plate is shown in Figure 3(b).

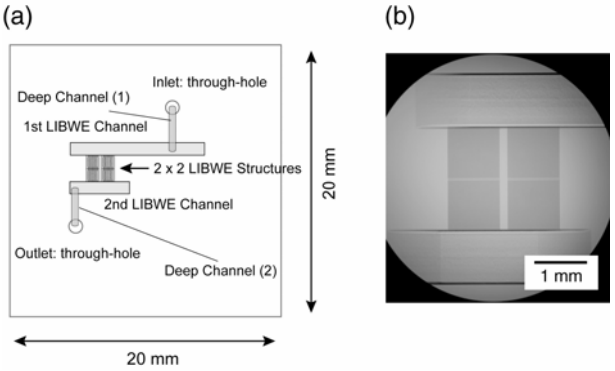

Fig. 3 (a) Schematic drawing of the structures on a silica glass plate. (b) An optical transmission micrograph of the microstructures.

3.2 Assembly of the device

Before assembly, microbeads were loaded into the microstructure by a combination of self- and force-loading. The bead suspension was sonicated for 5 to 10 s to make the distribution homogeneous prior to use. The typical concentration of beads was estimated to be 2 x 10^7 beads·mL^{-1} by using a Burker-Turk-type blood counting plate. Bead-containing suspension (3 μL) was dropped onto the microstructure by means of a micropipette. After leaving it for 5 min (avoiding complete dry-up), beads remaining outside the microstructure were gently force-loaded in the structure by rubbing them with a microscope cover glass. Excess beads were removed by a combination of wipes and rinsing in distilled water. The adhesion forces between the walls of the cavities and the beads were strong enough for the beads to remain fixed even after thorough rinsing in a beaker.

Thus prepared, the silica glass plate with a microstructure containing microbeads was sealed with a PDMS plate. As shown in the inset of Figure 4, these plates were fixed within a custom-made sample holder made from aluminium and acrylic plates. The fixation-pressure was adjusted by varying the length of the springs mounted on the screws. To avoid leakage, a fixation-pressure of approximately 12 kPa was added to the PDMS plate.

3.3 Flow behaviour in the microstructure

The microchannels (6-12 μm width, approx. 13 μm depth) used in our device were much smaller than those generally used in lab-on-a-chip systems (for example, 100 μm width and 40 μm depth). Considering the pressure loss Δp in tubes with circular cross section is inversely proportional to the square of diameter, d (eq. 1, l: length of the channel, η: the viscosity, <u>: the cross section-averaged flow rate), smaller size of microchannels must result in large pressure loss.

$$\Delta p = \frac{32\eta l \langle u \rangle}{d^2} \qquad (1)$$

Moreover, the channels have structure for fixing beads and microbeads are fixed inside. Therefore, solution flow itself is a difficult task in our device.

To keep solution flow, the pressure difference between inlet and outlet must be set higher than the pressure loss of channels. If flow rate is higher than that of the stationary flow, the pressure would continuously increase based on compression of the liquid.

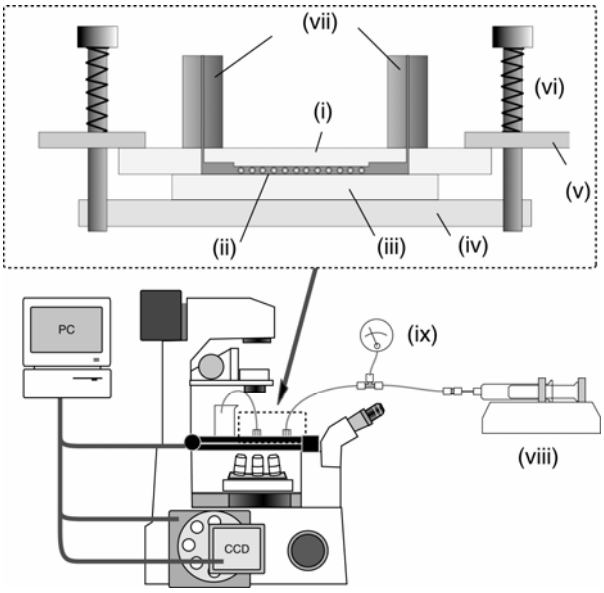

Fig. 4 Schematic illustration of the whole experimental setup including the fluorescence microscope. Inset: the cross-section of the assembled device, (i) silica glass plate with channels; (ii) microbeads fixed within the microstructure; (iii) PDMS plate; (iv) acrylic plate pressing PDMS (bottom plate of the sample holder); (v) aluminum top plate of the sample holder; (vi) springs and screws used for pressing PDMS; (vii) PEEK tubes; (viii) syringe pump system; (ix) pressure gauge.

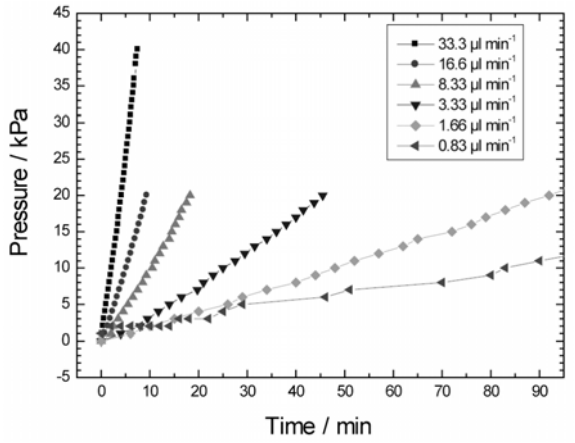

Fig. 5 Temporal evolution of pressure of the sample solution in the PEEK tube connecting syringe pump and chip without beads.

We studied the flow behaviour in the device by pumping an aqueous solution containing fluorescent dye (pyranine). First, we investigated the flow behavior in the device without beads. After solution appeared at the inlet, the liquid-air interface moved almost immediately from the inlet to the entrance of the microstructures and stopped there. The pressure never exceeded 4 kPa during this stage. Then the pressure started to increase monotonically (Fig. 5). At around 20 kPa, solution slowly started to fill the microstructures cavity by cavity and then reached the second LIBWE channel. Even when the solution appeared at the outlet, the pressure continued to increase monotonically until leakage occurred. The rates of the pressure increase ($\Delta p/\Delta t$) for various pump rates are listed in Table 1. The rates increased with pump rates. Generally, leakage occurred at over 40 kPa. If the PDMS plate was not pressed, leakage occurred at approximately 21 kPa.

Table 1 Rates of pressure increase in microstructures with and without beads present for various flow rates.

Flow rate [µl/min]	$\Delta p/\Delta t$ [kPa/min] w.o. beads	$\Delta p/\Delta t$ [kPa/min] with beads
33.3	5.28 ± 0.064	4.48 ± 0.061
16.7	2.26 ± 0.028	1.90 ± 0.033
8.33	1.12 ± 0.018	1.02 ± 0.015
3.33	0.45 ± 0.007	0.47 ± 0.009
1.66	0.22 ± 0.013	---
0.83	0.12 ± 0.002	---

Next, the solution flow in the device including the microbeads was examined. In the examined devices, 30% to 60% of the cavities were occupied by the beads. Similar pressure increases were observed (Table 1). Unlike the device without beads, the filling of the cavities is not homogeneous: some channels in the pattern filling faster than others. This inhomogeneity might result from inhomogeneous occupation of the cavities. Typically, liquid reached the other side of the microstructures at pressures of about 10 kPa. This pressure is less than the corresponding pressure in the beadless device. This difference could be from one or a combination of the following: (i) capillary force between beads and the cavity walls helps to transfer the solution to the other side, (ii) in the beadless device, pressed PDMS was inserted into the cavity. A higher pressure is necessary to expel the PDMS from the cavity. The insertion of PDMS into the channels was clearly observed at the edge of the LIBWE channel.

Figure 5 shows that flow rate must be minimized to achieve the quasi-stationary flow state. However, at such low flow rate, sample solution could not be supplied to microbeads immediately. Therefore, for practical analyses, we adopted two step protocol as followed. First, the solution was introduced to the device manually by using the "fast forward" function of the pump until the solution reached the second LIBWE channel. The flow rate during this process was about 30 µL·min^{-1}. When the solution reached the second LIBWE channel, the liquid pressure typically was about 10 kPa. Then, the solution flow with the rate of 2 µL·min^{-1} started. At this flow rate, the pressure increase for 20 min was 3 to 4 kPa. These values

correspond to 0.15 to 0.20 kPa·min^{-1}.

3.4 Capturing target molecules by microbeads in cavities

We examined the capturing performance of surface-modified microbeads arranged in the microstructures. First, fluorescein isothiocyanate (FITC) dissolved in a carbonate buffer (pH 10.1) was exposed to AEAPS-coated microbeads. In Figure 6(a) is an optical micrograph of the microstructure observed before the capturing experiment. AEAPS-coated microbeads were successfully arranged into the cavities, and 66% of the cavities were occupied by the beads. After sealing with a PDMS plate, the beads were exposed to a 0.26 mM FITC solution supplied via microchannels for 30 min under a quasi-stationary flow condition. After the exposure, the device was disassembled. Excess reagents were removed by rinsing with copious amounts of water. Figure 6(b) shows a fluorescent microscopic image of the same area of the microstructures shown in Figure 6(a). As described earlier, a filter set was chosen to detect the fluorescence signals from fluorescein derivatives. Clearly, the microbeads showed fluorescence from captured FITC. In the control experiment employing uncoated microbeads, no fluorescent beads were observed.

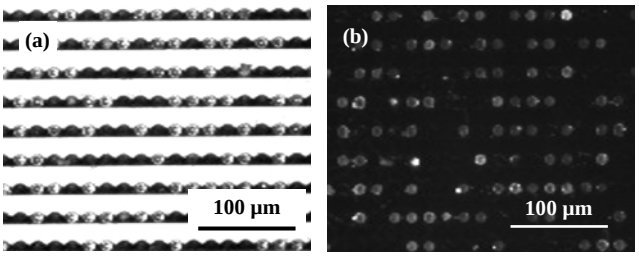

Fig. 6 Microscopic images of the microbeads arranged in the microstructure. (a) Transmission optical micrograph and (b) fluorescent micrograph of same area observed after 30 min reaction. Filter for excitation: 490 nm (FHWM 20 nm); filter for emission: 580 nm (FWHM 38 nm). Exposure time used was 8 s.

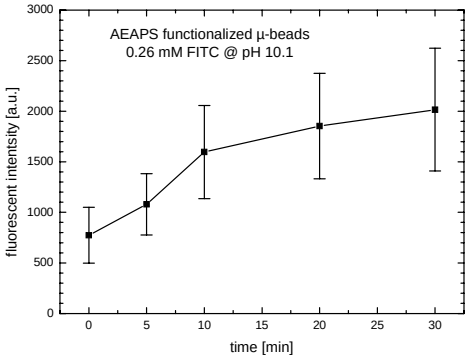

Fig. 7 Mean fluorescence intensities as a function of interaction time. An exposure time of 16 s was employed for all observations. The results are presented as means ± standard deviation.

Fluorescence intensities shown in various capturing conditions were studied. Figure 7 shows the fluorescence intensities of the beads as a function of reaction time. Each point was evaluated from the $280 < n < 450$ beads in the microstructures. As the figure shows, the mean fluorescence intensity increased gradually with reaction time. However, the increase became less pronounced for longer reaction times. On the basis of these data, we used a reaction time of 20 min for further experiments. At this reaction time, an signal to noise ratio (S/N) sufficient for subsequent evaluation was obtained.

The mean fluorescent intensities of microbeads as a function of FITC concentration are shown in Figure 8. Here, the number of the beads used for statistical evaluation was $75 < n < 300$, depending on the filling ratio at the microstructures. To evaluate the effect of background signals, the intensities of AEAPS-modified beads before exposure to FITC were evaluated by the same procedure as that for fluorescence intensities. In these experiments, the background intensity was estimated to be 288 ± 33. For concentrations higher than 83 μM, signal intensities increased with increasing FITC concentration. Given the flow rate of 2 μL/min and the reaction time of 20 min, the amount of FITC supplied to the microstructures was only 3.3 nmol. The FITC solution was supplied to 6400 cavities in the microstructures. Therefore, this value corresponds to 520 fmol for each cavity.

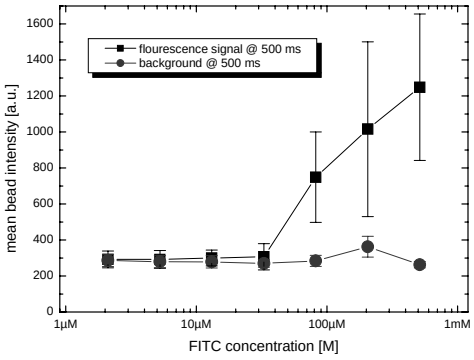

Fig. 8 Mean fluorescence intensity as a function of FITC concentration. An exposure time of 500 ms was employed in these experiments. The data are presented as means ± standard deviation.

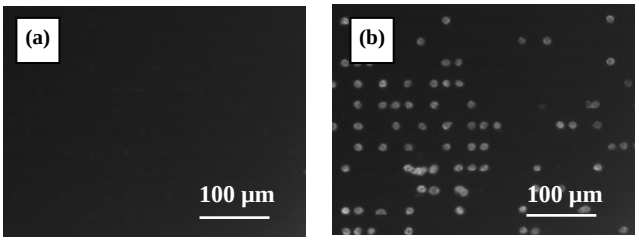

Fig. 9 Fluorescent micrographs obtained from avidin-immobilized PS beads (a) before and (b) after they were exposed to a flow of 2 μl/min biotin-4-fluorescine (4 μM in Tris-HCl buffer (10 mM)) for 20 min; filters; 16 s exposure.

Important characteristics of the present device include

its flexibility and reusability, as described earlier. We can exchange the bead set in the microstructure and reassemble the device. We removed the AEAPS-coated microbeads from the microstructure by sonication, and consequently arranged a different type of microbead, where avidin was immobilized on PS microbeads, in the same microstructure. Avidin is the protein generally used for fixing various probe molecules on patterned surfaces by the avidin-biotin method [28]. Figure 9(a) shows a fluorescent microscopic image obtained from avidin-coated PS microbeads. No fluorescence signal is detected here. Figure 9(b) depicts the same area of detail after the beads were exposed to a flow of 2 μl/min of biotin-4-fluorescein (4 μM) dissolved in a 10 mM Tris-HCl buffer for 20 min. This proved that not only glass microbeads but also polymer microbeads could be used in this device. Moreover, various capturing process such as hybridization of DNA can be used in this device.

4. Conclusion

We successfully demonstrated a new type of microbead sensor array incorporating microchannels fabricated by the LIBWE method. The array was characterized by means of pressure measurements at different flow rates. Surface-coated microbeads can be loaded into the microstructure to capture target molecules, as demonstrated by the typical capturing reaction systems of FITC-NH_2 and biotin-avidin. For FITC-NH_2 systems, the dependence of fluorescent bead intensity as a function of both interaction time and FITC concentration was studied. The chip can be reused for months without performance degradation.

Acknowledgments

This work was supported in part by the Industrial Technology Research Grant Program in '05 from the New Energy and Industrial Technology Development Organization (NEDO) of Japan. One author (T.G.) wishes to thank the Japanese Society for the Promotion of Science (JSPS) for the JSPS Postdoctoral Fellowship.

References

[1] K. F. Jensen, Chem. Eng. Sci., **56**, (2001) 293.
[2] H. Nakamura, Y. Yamaguchi, M. Miyazaki, H. Maeda, M. Uehara and P. Mulvaney, *Chem. Commun.*, (2002) 2844.
[3] J. Kobayashi, Y. Mori, K. Okamoto, R. Akiyama, M. Ueno, T. Kitamori and S. Kobayashi, Science, **304**, (2004) 1305.
[4] P. Reuse, A. Renken, K. Haas-Santo, O. Görke and K. Schubert, Chem. Eng. J., **101**, (2004) 133.
[5] M. A. Burns, B. N. Johnson, S. N. Brahmasandra, K. Handique, J. R. Webssterr, M. Krishnan, T. S. Sammarco, P. M. Man, D. Jones, D. Heldsinger, C. H. Mastrangelo and D. A. Burke, Science, **282**, (1998) 484.
[6] Y. Kikutani, M. Tokeshi, K. Sato and T. Kitamori, Pure Appl. Chem., **74**, (2002) 2299.
[7] P. Mela, S. Onclin, M. H. Goedbloed, S. Levi, M. F. García-Parajó, N. F. van Hulst, B. J. Ravoo, D. N. Reinhoudt and A. van den Berg, Lab on a Chip, **5**, (2005) 163.
[8]Micro Total Analysis System 2002, Y. Baba, S. Shoji, A. van den Berg ed. Kluwer Academic Publishers, Dordrecht, 2002.
[9] K. Sato, M. Tokeshi, H. Kimura and T. Kitamori, Anal. Chem., **73**, (2001) 1213.
[10] Y. Murakami, T. Endo, S. Yamamura, N. Nagatani, Y. Takamura and E. Tamiya, Anal. Biochem., **334**, (2004) 111.
[11] S. P. Fodor, J. L. Read, M. C. Pirrung, L. Styer, A. T. Lu and D. Solas, Science, **251**, (1991) 767.
[12] M. Schena and P. O. Brown, Science, **270**, (1995) 467.
[13] R. J. Fulton, R. L. McDade, P. L. Smith, L. J. Kienker and J. R. Kettman, Jr., Clin. Chem., **43**, (1997) 1749.
[14] J. D. Taylor, D. Briley, Q. Nguyen, K. Long, M. A. Iannone, M. S. Li, F. Ye, A. Afshari, E. Lai, M. Wanger, J. Chen and M. P. Weiner, Biotechniques, **30**, (2001) 661.
[15] S. Brenner, S. R. Williams, E. H. Vermaas, T. Stock, K. Moon, C. McCollum, J. I. Mao, S. Luo, J. J. Kirchner, S. Eletr, R.B. DuBridge, T. Burcham and G. Albercht, Proc. Natl. Acad. Sci. USA, **97**, (2000) 1665.
[16] S. Brenner, M. Johnson, J. Bridgham, G. Golda, D. H. Lloyd, D. Johnson, S. Luo, S. McCurdy, M. Foy, M. Evan, R. Roth, D. George, S. Eletr, G. Albecht, E. Vermaas, S. R. Williams, K. Moon, T. Burcham M. Pallas, T. B. DuBridge, J. Kichner, K. Fearon, J. Mao and K. Corcoran, Nat. Biotechnol., **18**, (2000) 630.
[17] D. R. Walt, Science, **287**, (2000) 451.
[18] J. A. Ferguson, F. J. Steemers and D. R. Walt, Anal. Chem., **72**, (2000) 5618.
[19] J. R. Epstein, J. A. Ferguson, K.-H. Lee and D. R. Walt, J. Am. Chem. Soc., **125**, (2003) 13753.
[20] Y. Kohara, H. Noda, K. Okano and H. Kambara, Nucleic Acids Res., **30**, (2002) e87.
[21] H. Noda, Y. Kohara and K. Okano and H. Kambara, Anal. Chem., **75**, (2003) 3250.
[22] M. F. Ali, R. Kirby, A. P. Goodey, M. D. Rodriguez, A. D. Ellington, D. P. Neikirk and J. T. McDevitt, Anal. Chem., **75**, (2003) 4732.
[23] Y.-S. Shon, A. Goodey, E. V. Anslyn, J. T. McDevitt, J. B. Shear and D. P. Neikirk, Biosensors, Bioelectron., **21**, (2005) 303.
[24] J. Wang, H. Niino and A. Yabe, Appl. Phys. A, **68**, (1999) 111.
[25] H. Niino, Y. Yasui, X. Ding, A, Narazaki, T. Sato, Y. Kawaguchi and A. Yabe, J. Photochem. Photobiol. A: Chem., **158**, (2003) 179.
[26] T. Gumpenberger, T. Sato, R. Kurosaki, A. Narazaki, Y. Kawaguchi and H. Niino, Chem. Lett., **35**, (2006) 218.
[27] X. Ding, Y. Kawaguchi, T. Sato, A. Narazaki and H. Niino, Langmuir, **20**, (2004) 9769.
[28] Avidin-Biochin Chemistry: A Handbook, M. Dean Savage, Pierce Chemical Co., 1992.

(Received: May 16, 2006, Accepted: November 8, 2006)